Chemical Engineering Journal 349 (2018) 829–837

Contents lists available at ScienceDirect

Chemical Engineering Journal

journal homepage: www.elsevier.com/locate/cej

Intensifying heat transfer in Fischer-Tropsch tubular reactors through the adoption of conductive packed foams

Laura Fratalocchi, Carlo Giorgio Visconti, Gianpiero Groppi, Luca Lietti, Enrico Tronconi*

Politecnico di Milano, Dipartimento di Energia, Via La Masa, 34, 20156 Milano, Italy

HIGHLIGHTS

- Highly conductive open-cell foams enhance heat transfer in packed-bed FTS reactors.
- Packed-foams enable running the FTS under severe conditions with excellent T-control.
- Thermal runaway occurs under mild conditions in conventional packed-bed reactor.
- Packed-foams provide an innovative solution to increase the catalyst inventory.
- Conductive packed foams are an efficient strategy for compact tubular reactor units.

GRAPHICAL ABSTRACT

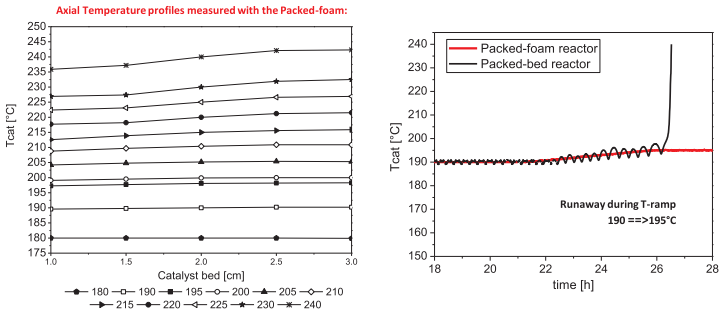

ARTICLE INFO

Keywords:
Fischer-Tropsch synthesis
Conductive structured catalysts
Packed foams
Heat transfer
Process intensification

ABSTRACT

The low-temperature Fischer-Tropsch synthesis is a strongly exothermic process wherein the temperature control is a crucial issue. In this work, we demonstrate experimentally for the first time the adoption of a Fischer-Tropsch tubular reactor (2.78 cm I.D.) loaded with a highly conductive open-cell aluminum foam packed with catalyst microspheres to enhance heat exchange. Accordingly, the performances of a highly active $Co/Pt/Al_2O_3$ catalyst packed into the metallic structure are assessed at industrially relevant operating conditions and compared with those obtained in a conventional randomly packed fixed-bed reactor. The structured catalyst reaches outstanding performances (duties in excess of 1300 kW/m^3 with CO conversions > 65%) with a remarkable temperature control. Almost flat axial temperature profiles are measured along the catalytic bed even under the most severe process conditions, showing the excellent ability of the "highly conductive packed-foam reactor" concept to manage the strong exothermicity of the reaction. In contrast, when the same experiment is carried out over the same $Co/Pt/Al_2O_3$ catalyst just randomly packed in the reactor, an abrupt increase of the catalyst temperature occurs already at low temperature, eventually leading to thermal runaway. The results herein collected prove the potential of conductive metal foams as enhanced reactor internals for the intensification of strongly exothermic processes in nonadiabatic tubular reactors. Furthermore, the "packed-foam" configuration also demonstrates the possibility to overcome the inherently limited catalyst inventory of the washcoated conductive structured reactors proposed so far, thus boosting the productivity per reactor volume.

* Corresponding author.
E-mail address: enrico.tronconi@polimi.it (E. Tronconi).

https://doi.org/10.1016/j.cej.2018.05.108
Received 21 March 2018; Received in revised form 17 May 2018; Accepted 18 May 2018
Available online 19 May 2018

1. Introduction

The low-temperature Fischer-Tropsch synthesis (FTS) is the well-known catalytic reaction which involves the hydrogenation of carbon monoxide over cobalt metal centers with the formation of long-chain hydrocarbons and water [1]. In the last decade, the interest in the FTS has been considerably renewed in view of exploiting both associated and remote natural gas fields to produce liquid fuels [2].

The reaction is carried out over supported cobalt-based catalysts at 20–30 bar and at temperatures below 240 °C. The FTS is a highly exothermic reaction due to a standard reaction enthalpy of $-165\ kJ/mol_{CO}$ combined with CO feed concentrations in excess of 25% and high CO conversions. Furthermore, the FT products distribution is notoriously sensitive to the catalyst temperature. In this regard, an inefficient temperature control would shift the product distribution to lighter hydrocarbons, i.e. methane, which is highly undesired. Accordingly the heat removal from the reactor is a key issue for the development of an intensified reactor technology [3].

Both fixed-bed and slurry reactors are commonly used for the FTS at the industrial scale [3]. In slurry bubble column reactors (SBCRs), the well-mixed liquid phase results in nearly isothermal operation that allows running the process at higher CO conversions per pass. However, catalyst particles for these reactors must be optimized to resist mechanical stress, attrition and hydrothermal effects. An efficient filtration system must be also provided for the separation of the liquid products from the catalyst particles [3,4]. Furthermore, the SBCR technology has a low specific productivity, which makes it convenient only at a very big scale.

The multitubular fixed-bed reactor (MTFBR) configuration is also used at the industrial scale [5], showing advantages like behavior close to plug flow conditions, high catalyst holdup, no need for catalyst separation and less difficult scale-up. However, weaknesses related to mass and heat transfer and pressure drop need to be addressed in view of the process intensification [3,4,6]. Mass transfer limitations may occur since large catalyst particles should be used to limit pressure drop across the catalyst bed [7–13]. The eggshell catalyst configuration may represent a promising solution even if the volumetric active density in the reactor is reduced with respect to the adoption of uniformly impregnated catalyst pellets [7,8].

Concerning the heat removal issue, the dominant pathway of the heat transfer in a MTFBR is associated with the tortuous flow path of the fluid phase. Heat transfer by static thermal conduction in the solid phase is, indeed, insignificant since only contact points are present between the catalyst particles and between the particles and the reactor walls [4]. This results in non-isothermal operation of the reactor with the presence of hot-spots and strong axial and radial T-gradients along the catalyst bed. This, in turn, may lead to a loss of selectivity, to a fast catalyst deactivation and, in the worst case, to the thermal runaway of the reactor [4].

At the industrial scale, such an issue is overcome by limiting the CO conversion per pass and recycling the unconverted syngas as well as a considerable fraction of the liquid reaction products at high flow rates. However, this increases pressure drops and makes the reactor less flexible to be scaled [6].

Nowadays, several research groups are focusing on the development of structured reactors with an improved thermal management suitable for small-scale GTL applications for remote or stranded gas sources [4,6,14–23]. In this regard, microchannel-based FT reactors are now commercially offered by Velocys [24]. The reactor is demonstrated to deliver approximately 175 barrels of FTS products per day [24]. The microchannel-design requires that the catalyst is housed within wave-like fin structures. The pressurized water coolant flowing inside cross-flow microchannels [24] efficiently removes the reaction heat. A major issue of the microchannel system is the fact that it introduces a totally new reactor technology, which is intrinsically more complex and expensive in comparison to the conventional multitubular fixed-bed reactor, a proven workhorse of the chemical and process industry during the last several decades.

As an alternative approach, structured catalysts with different geometries are proposed as viable alternatives for efficient heat removal in MTFBR applications [4,6,14–22]. In this regard, particularly promising results are obtained when the catalytic material is washcoated onto a spatially structured support substrate made of conductive materials [4,6,14–20]. This enables more isothermal operation of the reactor, thus reducing hot spots.

Different metallic supports with different geometries, such as commercial Al-foams and in-house made honeycomb monoliths (composed by alternated flat and corrugated foils) with different cell densities and made of both Fecralloy and Al, were widely studied for the FTS by Montes and coworkers at the University of the Basque Country [4,14,15]. They found that, regardless of the geometry, the adoption of metallic supports enables better performances than the corresponding powdered catalyst. Among the structures, monoliths with high thermal conductivity (made of Al) and high cell density (2300 cpsi) show improved heat exchange capabilities, thus representing a promising alternative to traditional packed-bed reactors [4]. On the contrary, the adoption of washcoated foams seems to be less feasible with respect to the other substrates [19,29]. This is mainly due to the several difficulties encountered during the coating process of the active phase onto these cellular structures. Furthermore, due to their low geometrical surface areas, very thick coatings are required to achieve sufficient catalyst loadings. As a result of the coating process, some catalytic material may be retained, partially blocking the macropores of the foam [14].

The potential of coated conductive monoliths in the FTS was actively investigated also in our group at Politecnico di Milano, Italy [3,6,25]. Visconti et al. [3] demonstrated by numerical simulations the ability of these substrates to manage the heat removal issue of the FTS and to guarantee an excellent temperature control. The heat transfer is strongly enhanced because the primary radial heat exchange mechanism is changed from flow dependent radial mixing in the gas phase associated with the tortuous flow path to static conduction within the thermally connected solid matrix of the honeycomb monolith [3,25], which makes it therefore also independent of the flow rate.

Another alternative concept of catalyst structures with enhanced heat transfer characteristics is represented by the conductive micro-fibrous entrapped catalysts (MFEC) developed by the Tatarchuk group at Auburn University, USA. They consist of sintered micron-sized metal fibers entrapping small catalyst particles [17,18], thus avoiding the need for washcoating. Flow heat transfer experiments demonstrated that MFECs made of conductive metals provided much greater effective thermal conductivities and wall heat transfer coefficients than conventional packed beds of particles. The adoption of MFEC allowed running the FTS at CO conversion levels of 50–80% [17,18].

A micro-structured reactor technology composed by eight parallel catalyst sections sandwiched between metallic cross-flow oil channels for heat exchange was also tested by Myrstad et al. [17] at NTNU, Norway. Each catalyst section was made of two foils with an etched deep pillar structure. The foils were stacked opposite to each other giving 800 μm channel height. The authors showed the capability of this system to efficiently remove the heat generated by a highly active Co-based catalyst working under severe FTS conditions [17].

In view of the development of compact and intensified Fischer–Tropsch reactors, closed cross flow structures (CCFS) packed with catalyst particle were recently proposed by Kapteijn and coworkers at TU Delft [21,22]. CCFSs consist of superimposed inclined corrugated sheets separated by flat sheets. It was numerically shown that the structured flow paths of the fluids through the packing roughly double the overall heat transfer properties of a randomly packed bed reactor. Furthermore, despite of a lower catalyst hold-up, the packed CCFS had a 25% higher C_{5+} productivity per reactor volume than the packed-bed [21,22].

In this work, we propose to enhance the heat transport properties of a FTS fixed bed reactor through the adoption of highly conductive open-cell metal foams packed with catalyst particles. These materials have been recently proposed by our group as a strategy to intensify heat transfer in strongly endo- and *exo*-thermic catalytic processes in tubular reactors [26–28]. Open-cell metal foams are particularly attractive structures since they have high porosity, low density, high mechanical strength and large surface area. They can be made of highly thermally conductive metals, such as Al or Cu. Combined with their continuous, thermally connected structure, this may offer a good potential for the improvement of the heat transfer properties of a FTS packed-bed reactor [26–28]. Open-cell foams in fact exploit the same conductive heat transfer mechanism of the monolithic substrates but, in addition, they have the advantage of enabling radial mixing within their structure, thus enhancing both the heat transfer and the flow uniformity [26–28].

It is also worth emphasizing that the conductive (static) heat transfer mechanism exploited within the packed-foam configuration is flow independent, in contrast e.g. with the governing mechanism in the recently proposed promising CCFS [21,22]: more flexible operation of the reactors is thus enabled.

In this paper, following the concept claimed in [26] and described in [27], we demonstrate for the first time the potential of a reactor configuration consisting of a conductive Al-foam packed with small catalyst particle to manage the severe temperature control requirement of the FT reaction. The adoption of the packed-foam configuration also overcomes the inherently limited catalyst inventory of the washcoated structured reactors proposed so far. This enables boosting the productivity per reactor volume of the FT reaction.

2. Experimental

2.1. Catalyst preparation and characterization

A home-made $Co/Pt/Al_2O_3$ catalyst containing 23 wt% of Co and 0.1 wt% of Pt (nominal loadings) is prepared following the procedure proposed by some of us in a recent publication [30]. The catalyst is supported on γ-Al_2O_3 microspheres (Sasol Puralox®, S_{BET} = 145 m^2/g, V_{pore} = 0.45 cm^3/g) with an average pellet diameter of 300 μm. Such a pellet size is a rational tradeoff preventing the onset of strong mass transfer limitations while granting acceptable pressure drops at the same time [7,8]. The first step of the preparation method is the stabilization of the γ-Al_2O_3 support with inactive cobalt aluminate species [2]. This is achieved upon high-T calcination (900 °C) of the alumina support after impregnation with 5.7 wt% Co. Cobalt used for this stabilization is defined "sacrificial" because it forms $CoAl_2O_4$ species which are not reduced under our activation conditions, and is thus inactive in the FTS [2]. Then, Pt is impregnated onto the stabilized support in a single incipient wetness impregnation (IWI) step using an aqueous solution of 3.4 wt% of $Pt(NH_3)_2{\cdot}(NO_2)_2$ in NH_4OH (Sigma Aldrich, 99 wt%). After that, an "active" cobalt loading of 18 wt% is added to the obtained material. For this purpose, the obtained material is impregnated four times with an aqueous solution of $Co(NO_3)_2{\cdot}6H_2O$ (Sigma Aldrich, 98.0 wt%). Each Pt and Co impregnation steps is followed by drying in static air at 120 °C for 2 h (heating rate 2 °C/min) and calcination at 500 °C for 4 h (heating rate 2 °C/min) [30].

The main properties of the $Co/Pt/Al_2O_3$ catalyst are summarized in Table 1.

Briefly, the BET area and the pore volume of the calcined catalyst are 59 m^2/g and 0.20 cm^3/g, respectively. The effective catalyst composition obtained by ICP-MS analysis, which is inclusive of the cobalt used for support stabilization, is in good agreement with the nominal Co and Pt loadings of the catalyst. The average cobalt particle size is determined via the Rietveld refinement of the patterns obtained with in-situ XRD measurements carried out in an X-ray diffractometer (Bruker D8 Advanced) equipped with a Co-Kα radiation source (λ = 1.78897 Å). An average Co_3O_4 crystallite size of 21 nm is calculated on the calcined sample, while an average Co^0 particle size of 9 nm is determined on the catalyst reduced in-situ at our activation conditions (H_2 treatment at 400 °C for 17 h, [30]). Notably, the estimated average Co^0 particle size is lower than the expected one based on the different density of Co oxide and metal ($d_{Co} \approx 0.75{\cdot}d_{Co3O4}$ [31]). This is likely due to the fact that the average size of the starting Co_3O_4 is slightly overestimated because of the partial overlapping of Co_3O_4 and $CoAl_2O_4$ reflections influencing the refinement, and/or to the sintering during the reduction step of the smallest Co oxides crystallites (undetectable by XRD) into bigger Co metal particles (well distinguishable in the XRD pattern). The degree of reduction (DOR) of the catalyst, calculated by considering only the amount of active cobalt added after the support stabilization, is monitored during the entire reduction step (H_2 treatment at 400 °C for 17 h) with in-situ magnetic measurements and is found to be 100% [30]. Further details on the characterization of the $Co/Pt/Al_2O_3$ catalyst after calcination and reduction will be revealed in a dedicated paper [30].

2.2. Packed-foam reactor

The open-cell aluminum foam with a nominal pore density of 40 ppi ($\varepsilon_{foam} \approx 0.906$; $d_{cell} \approx 2$ mm) was purchased from ERG Aerospace. As shown in Fig. 1, the shape of the foam is cylindrical with a length of 4 cm and a diameter of 2.78 cm, with tolerances of ± 0.030 cm. Notably, the diameter of the foam matches the nominal internal diameter (I.D.) of the stainless stell FT reactor used in the activity tests, so to ensure good contact and minimize dead space ("gap") between the tube and the cellular structure.

One axial through hole of 0.32 cm diameter is located at the centerline of the structure for the insertion of the stainless steel thermowell (1/8″ O.D.), protecting a sliding and a fixed J-type thermocouple (0.5 mm O.D.) (Figs. 1 and 2). The presence of the thermowell is not expected to affect the measured temperature profile being the thermowell made of stainless steel, whose intrinsic thermal conductivity is around 10 times lower than that of the aluminum of the foam (≈17 W/m/K vs 200 W/m/K [32]). Furthermore, its diameter is around 8 times smaller than that of the foam and its wall thickness is as low as 1 mm, which makes the axial thermal conductivity of the foam much greater than that of the thermowell.

Once the foam is loaded in the tubular reactor and the thermowell is positioned in the foam, the system is packed as schematically shown in Fig. 2. Initially, 5 g of α-Al_2O_3 pellets (d_{pellet} = 300 μm) are poured into the foam, thus forming a 1 cm deep layer. Then, 7.2 g of $Co/Pt/Al_2O_3$ catalyst diluted with a very small amount of α-Al_2O_3 (catalyst:α-Al_2O_3 = 6:1 w/w) with the same particle size are poured into the foam, thus forming a catalyst layer of 1.89 cm. Eventually, 5 g of α-Al_2O_3 pellets (d_{pellet} = 300 μm) are packed into the foam so to fill the last 1 cm of the structure. The resulting average catalyst volumetric density is

Table 1
Properties of the $Co/Pt/Al_2O_3$ catalyst.

BET area [m^2/g]	Pore volume [cm^3/g]	Co loading [wt%]	Pt loading [wt%]	dCo_3O_4[(a)] [nm]	dCo^0[(b)] [nm]	DOR[(b)] [%]
59	0.20	22.80 ± 0.59	0.110 ± 0.002	21	9	100

[(a)]dCo_3O_4 estimated after calcination; [(b)]dCo^0 and DOR calculated after in-situ reduction.

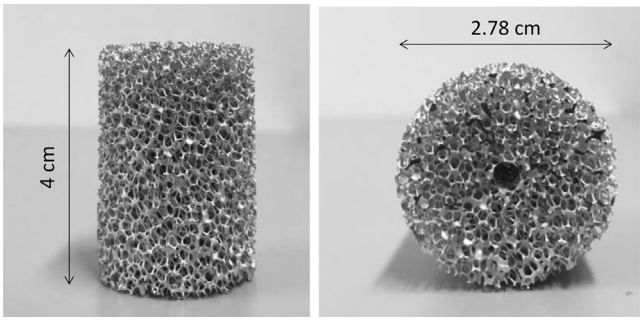

Fig. 1. Images of the open-cell aluminium foam.

0.63 g/cm^3, calculated as the ratio of the catalyst mass (7.2 g) to the reactor volume occupied by the catalyst bed (11.4 cm^3). The volumetric fraction of the catalyst inside the packed foam bed is found to be 0.48.

The total amount of pellets loaded into the foam corresponds exactly to the amount of pellets in a packed-bed with the same volume of the voids (cells) of the foam and ε_{PB} of 0.38. This clearly indicates that, probably due to the high d_{pore}/d_{pellet} ratio ($\approx$3.3), the small pellets can uniformly fill the voids of the foam structure, and the presence of the foam struts has negligible effects on the packing effectiveness.

2.3. Packed-bed reactor

In the case of the packed-bed reactor, 7.2 g of Co/Pt/Al_2O_3 catalyst are again randomly packed in the same tube used for the foam, but diluting with a large amount of α-Al_2O_3 (catalyst: α-Al_2O_3 = 1:1.7 w/w) pellets with the same particle size (d_{pellet} = 300 μm), so to form a catalyst bed with length of 4 cm, equal to the length of the foam ($\approx$4 cm). This leads to a catalyst volumetric density near 0.29 g/cm^3, i.e. almost half of that corresponding to the packed-foam reactor. Accordingly in the packed bed, at the same CO conversion level, the volumetric heat duty (kW/m^3) generated by the reaction is less than in the case of the packed foam.

2.4. Catalytic tests

The packed foam and the packed bed are tested in the FTS in a fully automated lab-scale rig [33] equipped with a stainless-steel tubular fixed-bed reactor 2.78 cm I.D., 85 cm long inserted in a three-zone split tube furnace (Carbolite, TVS/600).

The flow in the reactor is downward; the stream exiting the reactor passes a first vessel kept at 150 °C for waxes condensation and a second vessel cooled at 0 °C for the condensation of liquid aqueous and organic products. Incondensable gases leaving the vessels are periodically analyzed by an on-line GC (HP 6890) equipped with three columns and two detectors for the analysis of C_1–C_9 hydrocarbons (Al_2O_3-plot capillary column connected to a FID), of H_2, CH_4 and CO (molecular sieve column connected to a TCD) and of CO_2 (Porapak Q column connected to the same TCD detector). Condensable reaction products are analyzed daily by off-line GC (HP 6890) equipped with two FIDs and two HP-5 crosslinked 5% PH ME Siloxane capillary columns. This analytical procedure allows the detection of C_1–C_{49} hydrocarbons.

FTS runs were carried out at 180–240 °C, 25 bar, H_2/CO inlet molar ratio = 2.0, GHSV = 6410 cm^3(STP)/h/g_{cat}, inerts (N_2 + Ar) in the feed = 24 vol% for more than 800 h on stream.

Prior to exposing the sample to syngas, the catalyst is reduced in situ at 400 °C (heating ramp = 2 °C/min) for 17 h using 5000 cm^3(STP)/h/g_{cat} of H_2 (Sapio, 99.995 mol.%) at atmospheric pressure.

Process conditions are never changed before reaching steady-state conditions for both the catalyst activity and selectivity. In order to verify the achievement of steady state conditions, multiple on-line GC analysis are taken at fixed experimental conditions. The reactant conversion and the C_1–C_{49} products distribution (C_1–C_{49} paraffins, C_2–C_{17} olefins, CO_2) are periodically monitored during the experiments. Data are considered steady when the CO conversion (X_{CO}[%], Eq. (1)) and the selectivity (S_i[%], Eq. (2)) to the main FTS products vary within less than 5% in 24 h.

$$X_{CO}\ [\%] = \left(1 - \frac{F_{CO}^{out}}{F_{CO}^{in}}\right) \cdot 100 \tag{1}$$

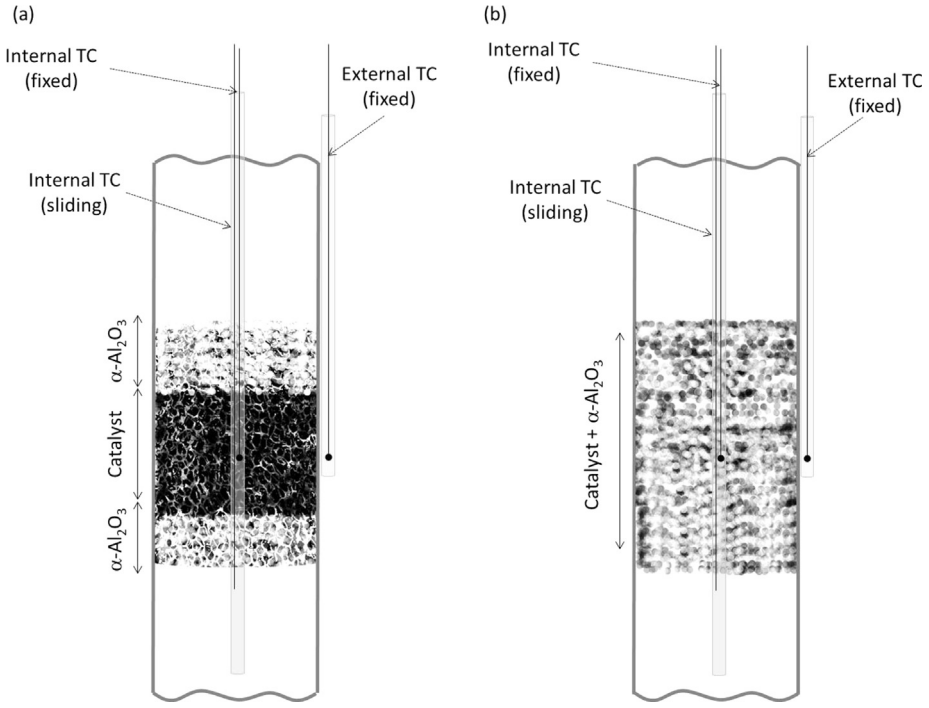

Fig. 2. (a) Scheme of the foam packed with catalyst pellets and loaded into the reactor (TC = thermocouple) and (b) of the packed-bed reactor.

$$S_i\ [\%] = \frac{F_i^{out} \cdot n_i}{\sum_{i}^{NP} (F_i^{out} \cdot n_i) + F_{CO2}^{out}} \cdot 100 \quad (2)$$

where F_i^{out} is the molar flow of the ith hydrocarbon species, F_{CO}^{in} is the molar flow rate of CO fed to the reactor, n_i is the carbon atom number of the ith species and NP (= 49) is the number of carbon atoms in the heaviest hydrocarbon identified at the reactor outlet. The selectivity to carbon dioxide is calculated as in Eq. (3):

$$S_{CO2}\ [\%] = \frac{F_{CO2}^{out}}{F_{CO}^{in} - F_{CO}^{out}} \cdot 100 \quad (3)$$

The specific productivity for C_{5+} hydrocarbons (Y_{C5+}) is calculated as in Eq. (4), where MW_i is the molecular weight of the ith species and w_{cat} the catalyst weight:

$$Y_{C5+}\ [g/h/g_{cat}] = \frac{\sum_{i \geq 5}^{NP} (F_i^{out} MW_i)}{w_{cat}} \quad (4)$$

The catalyst stability is verified by comparing the catalyst performances measured at 200 °C, 25 bar, H_2/CO inlet molar ratio = 2, GHSV = 6410 cm^3(STP)/h/g_{cat}, inerts (N_2 + Ar) in the feed = 24 vol%) at different Time on Stream (T.o.S.). These process conditions are defined as "standard conditions".

Carbon balances, calculated as moles of C contained in the reaction products divided by the moles of CO converted, always close within ± 10%, being typically within ± 5%.

The volumetric heat duty (Q) is calculated according to Eq. (5):

$$Q\left[\frac{kW}{m^3}\right] = \frac{-\Delta H_R^0 \cdot F_{CO}^{in} \cdot X_{CO}}{V_{cat}} = \frac{-\Delta H_R^0 \cdot F_{CO}^{in} \cdot X_{CO}}{\pi 4 \cdot (d_{reactor}^2 - d_{thermowell}^2) \cdot h_{cat}} \quad (5)$$

where ΔH_R^0 is the standard reaction enthalpy set to -165 kJ/mol$_{CO}$ and V_{cat} is the volume occupied by the catalyst in the reactor. The latter is calculated with a $d_{reactor}$ of 2.78 cm and a value of h_{cat} of 2 cm (packed-foam experiment) or 4 cm (packed-bed experiment).

Axial temperature profiles along the catalyst bed are measured by the sliding thermocouple inserted into the thermowell located at the centerline of the catalyst bed (Fig. 2). The axial temperature change (ΔT_{cat}) is defined as the difference between the maximum and the minimum temperature recorded along the catalyst bed. Another stainless steel thermowell (1/8″ O.D.), protecting a fixed J-type thermocouple (0.5 mm O.D.), is located at the outer wall of the reactor tube (T_{ext}), in correspondence of the mid point of the catalyst bed (Fig. 2). This allows to estimate an effective temperature difference for heat exchange (ΔT_{ext}), calculated as the difference between the temperature reading at the center of the catalyst bed and T_{ext} ($\Delta T_{ext} = T_{cat}^{centerline} - T_{ext}$).

Prior to the activity tests, a blank test was carried out at 200 °C, 25 bar, H_2/CO feed molar ratio = 2, GHSV = 6410 cm^3(STP)/h/g_{cat} and inerts (N_2 + Ar) in the feed = 24 vol%, so to identify the isothermal zone of the tubular reactor where locating the catalyst. To this end, the reactor was loaded with inert α-Al_2O_3 pellets and axial temperature profiles were measured along the reactor. A temperature difference less than 0.5 °C was obtained in 10 cm of the tube. Furthermore, no differences were noted between T_{ext} and the temperature reading at the center of the reactor (i.e. $\Delta T_{ext} \approx 0$ °C).

In the catalytic activity tests, the temperature inside the catalyst particle can be assumed constant as secured by the small value of the internal Prater number (see Appendix) [34]. Additionally, the absence of interphase (gas-solid) heat transport limitations is verified by applying the appropriate Mears' criterion (see Appendix) [35].

3. Results and discussion

3.1. Packed-foam reactor

The performances of the packed-foam reactor are shown in terms of CO conversion (Fig. 3) and selectivity to the main FTS products (Table 2). No information about the product distribution is given at 180, 190, 215, 230 and 240 °C because operation at these conditions lasted less than 24 h.

The results are reported as a function of the time on stream (T.o.S.). As already discussed, the catalyst activity was investigated for several hours (≈800 h) in a wide range of reaction temperatures between 180 and 240 °C, while keeping constant the other operating conditions: P = 25 bar, H_2/CO^{in} = 2 mol/mol, GHSV = 6410 cm^3(STP)/h/g_{cat}, inerts = 24 vol%.

As shown in Fig. 3, the catalyst is already active at temperatures lower than those conventionally used for the FTS (< 200 °C). In particular, the CO conversion measured at 180 and 190 °C was 3.7% and

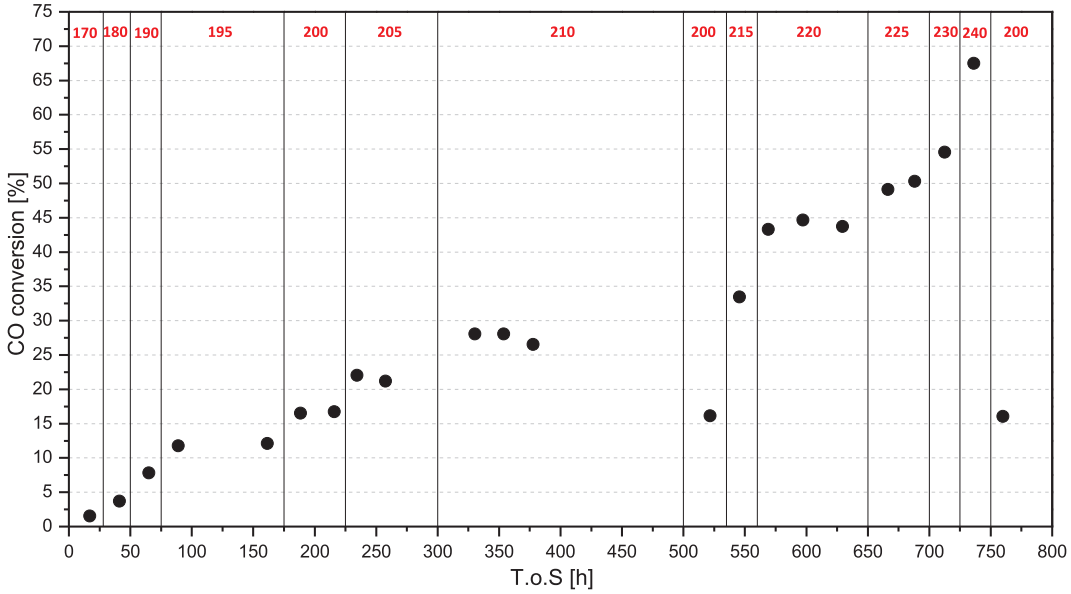

Fig. 3. Evolution of the CO conversion with time on stream (T.o.S.) at different temperatures (marked in red on the top of the graph, °C) during the experiments with the packed-foam. P = 25 bar, H_2/CO^{in} = 2 mol/mol, GHSV = 6410 cm^3(STP)/h/g_{cat}, inerts = 24 vol%. (For interpretation of the references to colour in this figure legend, the reader is referred to the web version of this article.)

Table 2
CO conversion and selectivity to the main FTS Products (CH_4, CO_2, C_2-C_4, C_{5+}, C_2-C_{17} olefins) calculated at different temperatures. The propylene/propane ($C_3^{//}/C_3$) and the volumetric heat duty (Q) are also shown. P = 25 bar, H_2/CO^{in} = 2 mol/mol, GHSV = 6410 cm^3(STP)/h/g_{cat}, inerts = 24 vol%.

T.o.S. [h]	T [°C]	X_{CO} [%]	S_{CH4} [%]	S_{CO2} [%]	S_{C2-C4} [%]	S_{C5+} [%]	$S^{olefins}$ (C_2-C_{17}) [%]	$C_3^{//}/C_3$ [−]	Q [kW/m^3]
41	180	3.7	3.6	–	–	–	–	–	80.6
65	190	7.8	6.7	–	–	–	–	–	161.2
162	195	12.1	8.4	0.5	11.5	76.6	19.2	1.2	243.9
216	200	16.5	10.9	0.6	13.8	71.6	15.1	0.8	332.5
258	205	21.2	14.6	0.8	14.2	67.4	12.0	0.6	427.3
378	210	28.1	17.3	1.0	14.5	65.2	8.4	0.4	566.3
546	215	33.5	19.6	1.4	–	–	–	–	675.1
597	220	44.7	21.0	2.0	15.4	59.3	6.0	0.3	900.9
688	225	50.3	23.5	2.8	16.0	56.3	4.6	0.2	1013.7
713	230	54.5	27.5	3.8	–	–	–	–	1098.4
736	240	67.5	33.3	7.1	–	–	–	–	1360.4

7.8%, respectively, while it reached 12.1% at 195 °C. This clearly indicates the high activity of the adopted Pt-promoted catalyst. When the reference conditions were reached (T = 200 °C), the CO conversion was 16.5% (Fig. 3). At this temperature the selectivity to CH_4, CO_2, C_2-C_4 and C_{5+} at 200 °C were 10.9, 0.6, 13.8 and 70.6%, respectively (Table 2).

Upon increasing the temperature from 205 to 210 and then to 215 °C, the CO conversion grew from 21.2% to 28.1% and then to 33.5% (Fig. 3). The CH_4 selectivity increased in the same T-range from 14.6% to 17.3% and to 19.6% (Table 2).

High CO conversions were obtained at temperatures above 215 °C: the catalyst reached 44.7% CO conversion at 220 °C, and 50.3% and 54.5% at 225 and 230 °C, respectively. At 240 °C, it reached 67.5% (Fig. 3). The CH_4 selectivity followed the same trend with values of 21.0, 23.5, 27.5 and 33.3% at 220, 225, 230 and 240 °C, respectively (Table 2).

The selectivity to CO_2 also increased on increasing temperature, going from a negligible value of 0.5% calculated at 195 °C to a high value of 7.1% estimated at 240 °C. This can be explained with the increase of the WGS activity of the catalyst at high CO conversions and hence at high-water concentration levels. Indeed, water is the most abundant FT product, as the oxygen atoms of CO are rejected as H_2O.

The selectivity to C_2-C_4 and C_{5+} hydrocarbons, as well as the selectivity to C_2-C_{17} olefins, was also significantly influenced by the reaction temperature (Table 2). In fact the selectivity to C_2-C_4 increased from 11.5% to 16.0% when the temperature was increased from 195 °C to 225 °C (Table 2).

The selectivity to C_{5+} hydrocarbons decreased upon increasing the temperature, going from 67.4 and 65.2% calculated at 205 °C and 210 °C, respectively, to 59.3% and 56.3% estimated at 220 °C and 225 °C (Table 2). These results are confirmed in Fig. 4, showing the typical Anderson–Schulz–Flory plot calculated at different temperatures. The ASF distributions have the typical positive and negative deviations for methane and C_2 hydrocarbons, respectively, and a change of slope for a carbon number around 8. The chain growth probability (α_{C15+}), estimated by considering the hydrocarbons with more than 15 carbon atoms, followed the same trend of the C_{5+} selectivity. In particular, α_{C15+} was 0.88 at 195 °C and around 0.87 at 200, 205 and 210 °C, and dropped to 0.84 at 220 °C and 225 °C (Fig. 4).

The olefin content in the products dropped upon increasing temperature. Accordingly, the selectivity to C_2-C_{17} olefins strongly decreased from 19.2% to 4.6%, when increasing the temperature from 195 °C to 225 °C. In line with this result, the propylene to propane ($C_3^{//}/C_3$) ratio decreased from 1.2 to 0.2 when going from 195 °C to 225 °C (Table 2).

These data are clear evidence that high temperatures result in high

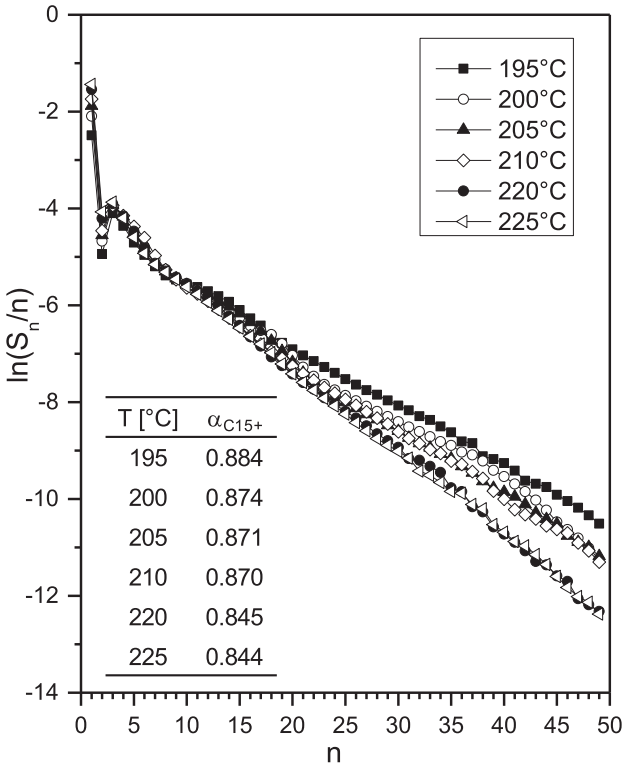

Fig. 4. Hydrocarbons ASF plots and α_{C15+} calculated at 195, 200, 205, 210, 220 and 225 °C. P = 25 bar, H_2/CO^{in} = 2 mol/mol, GHSV = 6410 cm^3(STP)/h/g_{cat}, inerts = 24 vol%.

catalyst activity. However, the increase of the temperature also results in a shift towards undesired light hydrocarbons. This can be explained by the fact that the hydrogenation rate is promoted by increasing temperatures, thus favoring the termination step over the growth step in the FTS chain growth mechanism [2].

The productivity of C_{5+} hydrocarbons (Y_{C5+}) is plotted in Fig. 5 as a function of the reaction temperature. It grows upon increasing temperature, indicating that the positive effect of the reaction temperature on the catalyst activity prevails on the observed negative effect on the products selectivity.

The volumetric heat duty (Q) calculated in the experiment with the packed-foam reactor increases with temperature (Table 2), being a function of the CO conversion. It starts from 80.6 kW/m^3 obtained at 180 °C, up to a remarkable value of 1360.4 kW/m^3 at 240 °C. To our knowledge, this is the first time in the scientific literature that such high-values are reported for the FTS reaction in a lab-scale apparatus. Notably, the volumetric heat duty at 230–240 °C may even be underestimated since the process selectivity is more shifted towards light hydrocarbons, especially CH_4 (S_{CH4} = 27.5–33.3%), and accordingly the standard FT reaction enthalpy of −165 kJ/mol_{CO} used in the calculation of Q is actually underrated, being the reaction enthalpy of methanation equal to −206 kJ/mol_{CO}. Notably, computed values of Q for the FTS (Table 2) are higher than typical values for selective oxidation reactions [36].

Fig. 6 shows the axial temperature profiles measured on the packed-foam at different temperatures (180–240 °C). Limited T-profiles along the catalyst bed are obtained at all the temperatures investigated, thus resulting in very small T-gradients even if in the presence of high volumetric heat duty. In this regard, the ΔT_{cat} is negligible at 180 °C and 190 °C, in line with the very low catalyst activity. Also in the 195–205 °C T-range, it is small ($\Delta T_{cat} \approx 1$ °C) although the CO conversion level increases up to 22%. On increasing the reaction temperature up to 210 °C and then to 215 °C, the T-gradients are only slightly

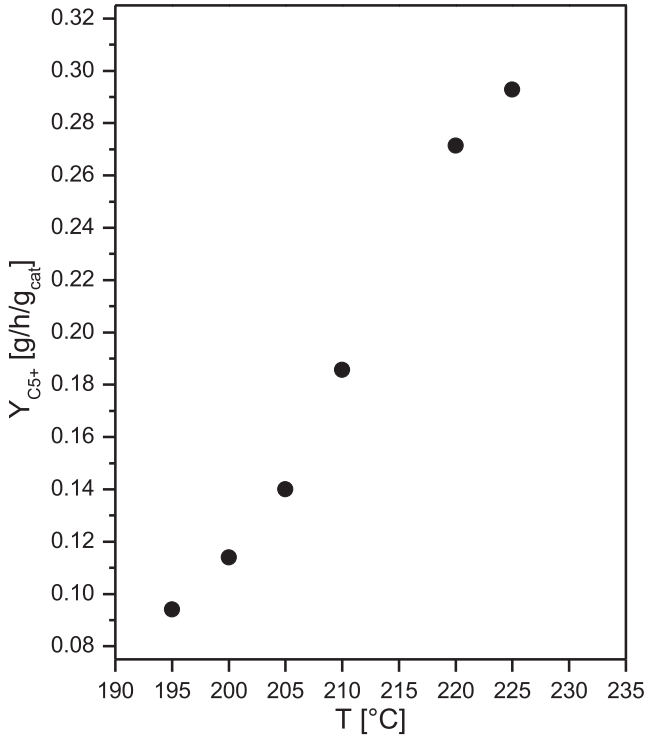

Fig. 5. Productivity of C_{5+} hydrocarbons as a function of the reaction temperature. P = 25 bar, H_2/CO^{in} = 2 mol/mol, GHSV = 6410 cm^3(STP)/h/g$_{cat}$, inerts = 24 vol%.

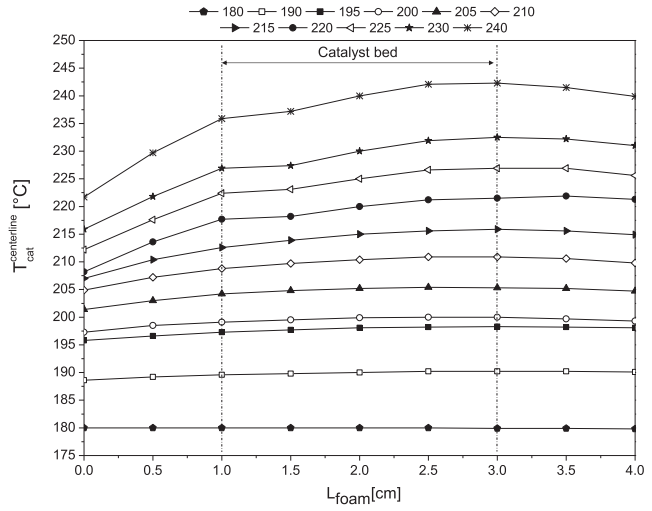

Fig. 6. Axial temperature profiles measured at different temperatures (T = 180, 190, 195, 200, 205, 210, 215, 220, 225, 230 and 240 °C) of the packed foam reactor by sliding the thermocouple located at the centerline of the foam. The position of the catalyst bed is also indicated. P = 25 bar, H_2/CO^{in} = 2 mol/mol, GHSV = 6410 cm^3(STP)/h/g$_{cat}$, inerts = 24 vol%.

affected, with a ΔT_{cat} of 2 and 3 °C, respectively. We recall that the CO conversion values at these temperatures are 28% and 33%, respectively. At 220 °C and 225 °C, with significant CO conversions of 44% and 50%, the ΔT_{cat} is still small and equals 4 °C and 4.5 °C, respectively. The most significant effect on the ΔT_{cat} is obtained at 230 °C and 240 °C when the CO conversion reaches the highest values (55% and 67.5%). Accordingly, the ΔT_{cat} becomes 5 °C and 6 °C, respectively.

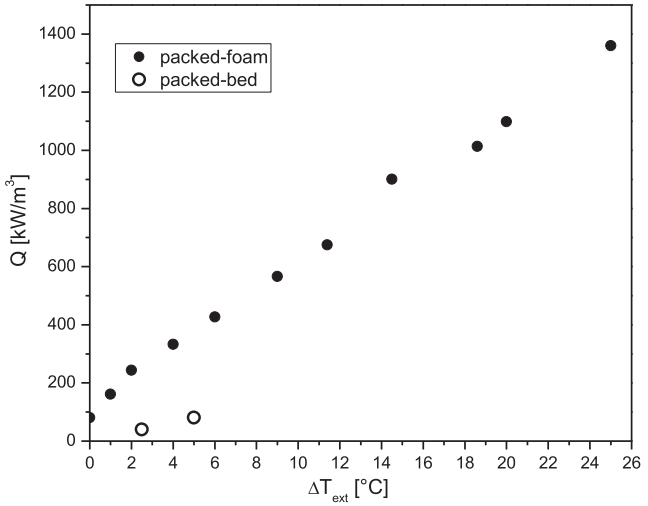

Fig. 7. Volumetric heat duty (Q) calculated during FTS experiments in the packed-foam as a function of the external (ΔT_{ext}) temperature difference. P = 25 bar, H_2/CO^{in} = 2 mol/mol, GHSV = 6410 cm^3(STP)/h/g$_{cat}$, inerts = 24 vol%.

Also ΔT_{ext} increases almost linearly with the increase of the volumetric heat duty (Fig. 7). Such a linear trend proves that: i) the oven is acting as a heat sink and not as a heat source, since the heating elements are set to temperatures well below $T_{cat}^{centerline}$ and T_{ext}; ii) ill-defined heat exchange conditions from the external skin of the reactor tube to the oven do not result in major anomalies affecting heat transfer within the reactor (including the likely limiting contribution of the heat resistance close to the internal reactor wall), which is the focus of the present investigation.

Noteworthy, although the catalyst was tested for several hours (≈800 h), which is unusual for lab-scale runs, and frequently varying the process conditions, it was found to be very stable with the Time on Stream (T.o.S.) (Fig. 3). In fact, the CO conversion measured by replicating the standard conditions at different T.o.S. (200, 520 and 760 h) was always around 16%. This is particularly interesting since the catalyst worked under severe conditions (i.e. high P_{H2O}/P_{H2} in particular in the second half of the catalyst bed [2]) for more than 200 h.

We believe that this is a further indication of the excellent heat transfer properties of the packed foam reactor, which prevents the deactivation of the catalyst by avoiding strong temperature gradients in the catalyst bed.

3.2. Packed-bed reactor

The CO conversion values measured at 180 °C and 190 °C were the same obtained in the packed-foam reactor. The catalyst performances could be recorded only at these low temperatures, however, since a thermal runaway occurred as soon as the catalyst reached 195 °C. As shown in Fig. 8, in fact, the catalyst temperature became unstable even during the temperature ramp from 190 to 195 °C, with fluctuations, signals of incipient reactor instability that increased gradually up to the onset of the thermal runaway. The catalyst temperature measured in the packed-foam reactor configuration was flat thanks to the presence of the highly conductive foam which strongly favors the reaction heat removal (Fig. 7). In contrast, the catalyst bed in the packed-bed reactor configuration resulted strongly not isothermal with axial temperature gradients along the catalyst bed (ΔT_{cat}) of 5 °C (at 180 °C) and 9 °C (at 190 °C). The external temperature gradient (ΔT_{ext}) went from 2.5 to 5 °C when the process temperature was set to 180 and 190 °C, respectively.

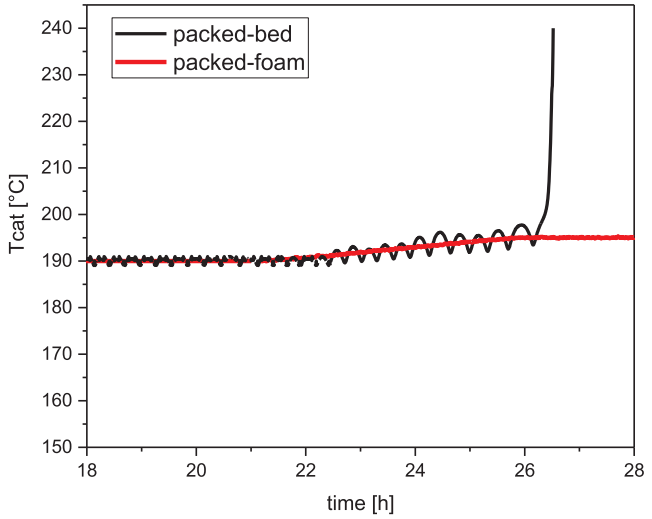

Fig. 8. Temporal evolution of the catalyst temperature measured at the center of the catalyst bed during the T-ramp from 190 to 195 °C: packed foam (red line) and packed-bed reactor (black line). P = 25 bar, H_2/CO^{in} = 2 mol/mol, GHSV = 6410 cm^3(STP)/h/g_{cat}, inerts = 24 vol%. (For interpretation of the references to colour in this figure legend, the reader is referred to the web version of this article.)

Noteworthy, the packed bed reactor worked under milder process conditions (the catalyst volumetric density was halved) if compared with the packed-foam reactor. All the results shown in this work are therefore clear evidence of the efficacy of the highly conductive packed-foam configuration in removing the heat generated by the strongly exothermic FTS. These results clearly indicate that also under severe conditions (i.e. high reaction heat release) the adoption of the packed-foam reactor enables running the FTS process with an outstanding temperature control.

The comparison with the experiment in the packed foam, therefore, clearly emphasizes the strongly positive effect of the conductive cellular foam structure in effectively controlling the strong exothermicity of the Fischer-Tropsch synthesis in tubular reactors, already at the laboratory scale.

4. Conclusions

Temperature management is a key challenge for the intensification of the Fischer-Tropsch process in multitubular fixed-bed reactors. In this regard, herein we show for the first time that the adoption of open-cell foams made of a thermally conductive material as reactor internals can be an effective solution to enhance the overall heat transfer performances of packed-bed FTS reactors. Our data confirm that, thanks to the adoption of the conductive foams, the mean temperature inside the reactor can be controlled much better providing new operating windows, which are not accessible using the conventional packed-bed reactor technology. The conductive packed-foams enable in fact running the FT reaction under severe conditions (i.e. high CO conversion and large heat duty) with an intensified temperature control. Indeed, in a crucial comparative experiment the conventional packed-bed reactor, although operated under milder conditions (i.e. the catalyst density was halved with respect to the foam), experienced thermal runaway already at very low temperatures and CO conversions, i.e. with limited release of reaction heat. These results are a direct indication that the heat exchange is significantly enhanced thanks to the structured conductive substrate of the foam.

In more general terms, it is worth mentioning that highly conductive packed-foams also represent an innovative solution to increase the catalyst inventory in structured tubular reactors, since the catalyst load which can be packed in the open-cell foam is much greater than the amount which can be loaded by washcoating the same foam. In this way, the productivity per reactor volume can be boosted. In addition, “packing” the foam means overcoming all the problems linked to the coating process, to the catalyst loading and unloading in the reactor, and to the replacement of the spent catalyst. Furthermore, the packed-bed configuration allows exploiting the most effective heat transfer mechanisms available, i.e. conduction within the highly conductive structured substrate in the bulk of the bed and convection due to local mixing in the packed bed at the boundary between the bed and the tube wall [27]. Accordingly, the concept of conductive packed foams may provide an effective design strategy in the case of compact tubular reactor units for strongly exothermic (as well as endothermic) processes.

The results obtained in this work at the lab scale clearly prove that the adoption of highly conductive packed-foams is an innovative strategy to boost the productivity per reactor volume of the reactions under kinetic control, while granting at the same time enhanced heat transfer performances and safe operation of the reactor. On the other hand, we recognize the need for an assessment of the system performances under fully representative conditions, e.g. in a jacketed single-tube pilot reactor with dimensions suitable to mimic the operation of technical multitubular reactors. This is indeed the goal of our future research efforts aimed at the scale up of the packed foam reactor concept for the Fischer-Tropsch synthesis.

Keeping at the lab-scale the adoption of conductive cellular internals can be exploited for lab-scale kinetic studies of strongly exothermic catalytic reactions, as it enables an excellent temperature control even under severe operating conditions which would not be otherwise accessible, thus extending the feasible range of kinetic investigations.

Acknowledgment

The research leading to these results has received funding from the European Research Council under the European Union’s Horizon 2020 research and innovation program (Grant Agreement no. 694910/INTENT).

Appendix A

A.1. Absence of internal temperature gradients

The temperature inside the catalyst particle can be assumed constant since the criterion shown in Eq. (A.1), which depends on the dimensionless activation energy γ, the internal Prater number β_i and the Wheeler–Weisz modulus $\eta\phi^2$, is satisfied [34,35]:

$$\gamma\cdot\beta_i\cdot(\eta\cdot\phi^2) = \left(\frac{Ea}{R\cdot T}\right)\left(\frac{(-\Delta H_R^0)\cdot r_{CO}^0\cdot\rho_{cat}\cdot l_{cat}^2}{\lambda_{cat}\cdot T}\right) = 0.006 < 0.05 \quad (A.1)$$

where T is the maximum temperature reached during the experiments (513 K), R is the gas constant (8.314 J/mol/K), Ea and r_{CO}^0 are the apparent activation energy (132 kJ/mol) and the consumption rate ($5.34\cdot10^{-5}$ mol/s/g_{cat}) calculated at the reactor inlet by fitting the Yates-Satterfield rate expression [37] to the CO conversion data. $\Delta H_R^0$is the standard reaction enthalpy (-165 kJ/mol), ρ_{cat} is the catalyst particle density ($1.32\cdot10^6$ g_{cat}/m^3), l_{cat} is the characteristic catalyst length ($D_{pellet}/6 = 5\cdot10^{-5}$ m) and λ_{cat} is the catalyst thermal conductivity (0.3 W/m/K).

A.2. Absence of external interphase (gas-solid) heat transfer limitations

External interphase (gas-solid) heat transport limitations can be neglected due to the fact that the Mears criterion (Eq. (A.1)) [35] is satisfied:

$$\left(\frac{Ea\cdot(-\Delta H_R^0)\cdot r_{CO}^0\cdot\rho_{cat}\cdot l_{cat}}{h\cdot R\cdot T^2}\right) = 0.007 < 0.05 \tag{A.1}$$

where T is the maximum temperature reached during the experiments (513 K), R is the gas constant (8.314 J/mol/K), Ea and r_{CO}^0 are the apparent activation energy (132 kJ/mol) and the consumption rate ($5.34\cdot10^{-5}$ mol/s/g_{cat}) calculated at the reactor inlet by fitting the Yates-Satterfield rate expression [36] to the CO conversion data. ΔH_R^0 is the standard reaction enthalpy (−165 kJ/mol), ρ_{cat} is the catalyst particle density ($1.32\cdot10^6$ g_{cat}/m^3) and l_{cat} is the characteristic catalyst length ($D_{pellet}/6 = 5\cdot10^{-5}$ m). The gas-solid heat transfer coefficient, h (5032 W/m^2/K) is found from the Nusselt number ($Nu = \frac{h\cdot l_{cat}}{\lambda}$, where λ is the thermal conductivity of the gas phase (0.11 W/m/K)), and Nu is estimated with a packed bed correlation based on bed porosity ($Nu = \frac{1.31\cdot Re^{1/3}\cdot Pr^{1/3}}{\varepsilon_{PB}}$, with $\varepsilon_{PB} = 0.38$) [34].

References

[1] M.E. Dry, Catal. Today 71 (2002) 227–241.
[2] L. Fratalocchi, C.G. Visconti, L. Lietti, G. Groppi, E. Tronconi, E. Roccaro, R. Zennaro, Catal. Sci. Technol. 6 (2016) 6431–6440.
[3] C.G. Visconti, E. Tronconi, G. Groppi, L. Lietti, M. Iovane, S. Rossini, R. Zennaro, Chem. Eng. J. 171 (2011) 1294–1307.
[4] D. Merino, O. Sanz, M. Montes, Chem. Eng. J. 327 (2017) 1033–1042.
[5] S.T. Sie, M.M.G. Senden, H.M.H. Van Wechem, Catal. Today 8 (1991) 371–394.
[6] C.G. Visconti, E. Tronconi, L. Lietti, G. Groppi, P. Forzatti, C. Cristiani, R. Zennaro, S. Rossini, Appl. Catal. A 370 (2009) 93–101.
[7] L. Fratalocchi, C.G. Visconti, L. Lietti, E. Tronconi, U. Cornaro, S. Rossini, Catal. Today 246 (2015) 125–132.
[8] L. Fratalocchi, C.G. Visconti, L. Lietti, E. Tronconi, S. Rossini, Appl. Catal. A 512 (2016) 36–42.
[9] E. Iglesia, S.C. Reyes, R.J. Madon, S.L. Soled, Adv. Catal. 39 (1993) 221–302.
[10] E. Iglesia, Appl. Catal. A 161 (1997) 59–78.
[11] M.F.M. Post, A.C. Van'tHoog, J.K. Minderhoud, S.T. Sie, J. Am. Inst. Chem. Eng. 35 (1989) 1107–1114.
[12] A.M. Hilmen, E. Bergene, O.A. Lindvåg, D. Schanke, S. Eri, A. Holmen, Catal. Today 69 (2001) 227–232.
[13] F. Kapteijn, R.M. Deugd, J.A. Moulijn, Catal. Today 105 (2005) 350–356.
[14] L.C. Almeida, F.J. Echave, O. Sanz, M.A. Centeno, G. Arzamendi, L.M. Gandìa, E.F. Sousa-Aguiar, J.A. Odriozola, M. Montes, Chem. Eng. J. 167 (2011) 536–544.
[15] L.C. Almeida, O. Sanz, D. Merino, G. Arzamendi, L.M. Gandìa, M. Montes, Catal. Today 215 (2013) 103–111.
[16] R. Mystrad, S. Eri, P. Pfeifer, E. Rytter, A. Holmen, Catal. Today 147S (2009) S301–S304.
[17] M. Sheng, H. Yang, D.R. Cahela, W.R. Yantz Jr., C.F. Gonzales, B.J. Tatarchuck, Appl. Catal. A 445–446 (2012) 143–152.
[18] M. Sheng, H. Yang, D.R. Cahela, B.J. Tatarchuck, J. Catal. 281 (2011) 254–262.
[19] M. Lacroix, L. Dreibine, B. de Tymowski, F. Vigneron, D. Edouard, D. Begin, P. Nguyen, C. Pham, S. Savin-Poncet, F. Luck, M.J. Ledoux, C. Pham-Huu, Appl. Catal. A 397 (2011) 62–72.
[20] I. Graf, A.K. Ruhl, B. Kraushaar-Czarnetzki, Chem. Eng. J. 244 (2014) 234–242.
[21] N. Hooshyar, D. Vervloet, F. Kapteijn, P.J. Hamersma, R.F. Mudde, J.R. van Ommen, Chem. Eng. J. 207–208 (2012) 865–870.
[22] B. Kaskes, D. Vervloet, F. Kapteijn, J.R. van Ommen, Chem. Eng. J. 283 (2016) 1465–1483.
[23] S. Saeidi, M.K. Nikoo, A. Mirvakili, S. Bahrani, N.A.S. Amin, M.R. Rahimpour, Rev. Chem. Eng. 31 (3) (2015) 209–238.
[24] R.J. Kee, C. Karakaya, H. Zhu, Proc. Combust. Inst. 36 (2017) 51–76.
[25] M. Iovane, R. Zennaro, P. Forzatti, G. Groppi, L. Lietti, E. Tronconi, C.G. Visconti, S. Rossini, E. Mignone, Pat. Appl. WO/2010/130399.
[26] G. Groppi. E. Tronconi, C.G. Visconti, A. Tasso, R. Zennaro, Pat. Appl. WO/2015/033266.
[27] C.G. Visconti, G. Groppi, E. Tronconi, Catal. Today 273 (2016) 178–186.
[28] E. Tronconi, G. Groppi, C.G. Visconti, Curr. Opin. Chem. Eng. 5 (2014) 55–67.
[29] C. Pham-Huu, B. Madani, M. Lacroix, L. Dreibine, M.J. Ledoux, S. Savin-Poncet, J. Bousquet, D. Schweich, Int. Pat. Appl. (2007) WO 2007/000506 A1.
[30] L. Fratalocchi, C. G. Visconti, L. Lietti, N. Fischer, M. Claeys, in preparation.
[31] D. Schanke, S. Vada, E.A. Blekkan, A.M. Hilmen, A. Hoff, A. Holmen, J. Catal. 156 (1995) 85–95.
[32] F.P. Incropera, D.P. De Witt (Eds.), Introduction to Heat Transfer, Wiley, 1996.
[33] C.G. Visconti, L. Lietti, P. Forzatti, R. Zennaro, Appl. Catal. A 330 (2007) 49–56.
[34] D. Vervloet, F. Kapteijn, J. Nijenhuis, J. Ruud van Ommen, Catal. Sci. Technol. 2 (2012) 1221–1233.
[35] D.E. Mears, J. Catal. 20 (1971) 127–131.
[36] G. Eigenberger, Fixed Bed Reactors, Ullmann's Encyclopedia of Industrial Chemistry, 84 (1992), pp. 199–238.
[37] I.C. Yates, C.N. Satterfield, Energy Fuels 5 (1991) 168–173.